PERGAMON

Carbon 37 (1999) 1379–1389

CARBON

Modification of the surface chemistry of activated carbons

J.L. Figueiredo*, M.F.R. Pereira, M.M.A. Freitas, J.J.M. Órfão

Laboratório de Catálise e Materiais, Departamento de Engenharia Química, Faculdade de Engenharia da Universidade do Porto, 4099 Porto, Portugal

Received 8 September 1998; accepted 18 December 1998

Abstract

A NORIT activated carbon was modified by different chemical and thermal treatments (including oxidation in the gas and liquid phases) in order to obtain materials with different surface properties. Several techniques were used to characterize these materials including nitrogen adsorption, chemical and thermal analyses, XPS, TPD and DRIFTS. The results obtained by TPD agree quantitatively with the elemental and proximate analyses of the oxidized materials, and qualitatively with the observations by DRIFTS. A simple deconvolution method is proposed to analyse the TPD spectra, allowing for the quantitative determination of the amount of each functional group on the surface. A multiple gaussian function has been shown to fit the data adequately, the parameters obtained for each fit matching very well the features observed in the experimentally determined TPD spectra.

It is shown that gas phase oxidation of the carbon increases mainly the concentration of hydroxyl and carbonyl surface groups, while oxidations in the liquid phase increase especially the concentration of carboxylic acids. © 1999 Elsevier Science Ltd. All rights reserved.

Keywords: A. Activated carbon; B. Oxidation; C. TPD; D. Surface oxygen complexes

1. Introduction

Carbon materials are finding an increasing number of applications in catalysis, either as supports for the active phases, or as catalysts on their own. Their performance is determined both by their texture and surface chemistry [1].

In the case of activated carbons, the texture may be adapted to suit the situation by adequate choice of the activation procedure. In particular, it is possible to prepare carbons with different proportions of micro, meso and macropores [2].

On the other hand, the nature and concentration of surface functional groups may be modified by suitable thermal or chemical post-treatments. Oxidation in the gas or liquid phase can be used to increase the concentration of surface oxygen groups, while heating under inert atmosphere may be used to selectively remove some of these functions. Carboxyl, carbonyl, phenol, quinone, and lactone groups, have been identified on carbon surfaces [3,4].

A variety of experimental techniques has been used to characterize these functional groups, such as chemical titration methods [3,5–7], temperature-programmed desorption (TPD) [8–10], X-ray photoelectron spectroscopy (XPS) [11,12] and infra-red spectroscopy methods (FTIR, DRIFTS) [8,13–15].

The chemical titration methods, such as proposed by Boehm [3,5], are especially useful when used in combination with other techniques [16]; however, they are not practical when dealing with small samples. In addition, these methods fail to account for a large proportion (as high as 50%) of the total oxygen content of carbon materials [17].

XPS is a surface technique which will provide an estimate of the chemical composition of the few uppermost layers of the material. In order to get further insight into the nature of the functional groups on the surface, a reconstruction of the O1s peak can be performed [18]. The reconstruction of the C1s region is generally more difficult, not only as a result of the broadness of the peak, but also because it is necessary to make an assumption concerning its nature after oxidation, namely if the surface graphite-like structure remains unchanged or not. This will affect the curve fitting procedure, an asymmetric peak shape

*Corresponding author.

0008-6223/99/$ – see front matter © 1999 Elsevier Science Ltd. All rights reserved.
PII: S0008-6223(98)00333-9

being needed for the graphite-like structure, while a gaussian peak is required for an aliphatic structure [19].

Infra-red spectroscopic methods can be applied only to highly oxidized carbons, otherwise the intensity of the absorption bands is not sufficient. Diffuse Reflectance FTIR (DRIFTS) is preferable, to avoid the problems caused by sample dilution, and a recent study has shown the usefulness of the technique to monitor the surface functionalities that develop under oxidizing conditions [14]. The interpretation of the spectra is complicated by the fact that each group originates several bands at different wavenumbers, therefore each band may include contributions from various groups (cf. Table 1).

Temperature-programmed methods have become rather popular. Surface oxygen groups on carbon materials decompose upon heating by releasing CO and CO_2 at different temperatures. There is some confusion in the literature with respect to the assignment of the TPD peaks to specific surface groups, as the peak temperatures may be affected by the texture of the material, the heating rate and the geometry of the experimental system used [20–22]. However, some general trends can be established as summarized in Fig. 1. Thus, a CO_2 peak results from carboxylic acids at low temperatures, or lactones at higher temperatures; carboxylic anhydrides originate both a CO and a CO_2 peak; phenols, ethers, and carbonyls (and quinones) originate a CO peak. In general, the TPD spectra obtained with carbon materials show composite CO and CO_2 peaks which must be deconvoluted before the surface composition can be estimated.

Thus, in general the quantitative analysis of the surface functional groups is not straightforward. In the present work, activated carbons were modified by thermal or chemical post-treatments in order to obtain materials with different surface properties which were then characterized by different techniques, in an attempt to determine quantitatively the amount of each chemical function on the surface. A simple deconvolution method is proposed to analyse the TPD profiles, and the results obtained seem to validate this procedure.

2. Experimental

A NORIT ROX 0.8 activated carbon (pellets of 0.8 mm diameter and 5 mm length) was used as supplied and after different oxidation treatments: in the gas phase, with 5% O_2 (in N_2) at 698 K for different times in order to achieve the desired burn-off (B.O.), or with 50% N_2O (in N_2) for 8 h at 773 K; and in the liquid phase, with 5M nitric acid at the boiling temperature for 6 h, or with 10 M H_2O_2 at room temperature. The materials oxidized in the liquid phase were subsequently washed with distilled water until neutral pH, and dried in an oven at 383 K for 24 h. The following samples were prepared: A1-original carbon; A2–A1 oxidized with 5% O_2 for 3 h at 698 K (B.O.=8.7%); A3–A1 oxidized with 5% O_2 for 6 h at 698 K (B.O.= 12.5%); A4–A1 oxidized with 5% O_2 for 10 h at 698 K (B.O.=21.5%); A5–A1 oxidized with 5% O_2 for 20 h at 698 K (B.O.=41.5%); A6–A4 treated under nitrogen at 873 K for 1 h; A7–A4 treated under nitrogen at 1023 K for 1 h; A8–A4 treated under nitrogen at 1373 K for 1 h; A9–A1 oxidized with 50% N_2O for 8 hours at 773 K (B.O.=21%); A11–A1 oxidized with 5M nitric acid for 6 h at boiling temperature; A12–A1 oxidized with 10 M H_2O_2.

The textural characterization of the materials was based on the N_2 adsorption isotherms, determined at 77 K with a Coulter Omnisorp 100 CX apparatus. The micropore volumes and mesopore surface areas were determined by the t-method, using the standard isotherm for carbon materials proposed by Reinoso et al. [27]. The adsorption data were also analysed with the Dubinin equation. When a type IV deviation occurred, two microporous structures were taken into account, and the corresponding volumes, W_{01} and W_{02}, were calculated [28]. The Stoeckli equation

Table 1
IR assignments of functional groups on carbon surfaces (adapted from Ref. [14])

Group or functionality	Assignment regions (cm^{-1})		
	1000–1500	1500–2050	2050–3700
C–O in ethers (stretching)	1000–1300		
Alcohols	1049–1276		3200–3640
Phenolic groups:			
C–OH (stretching)	1000–1220		
O–H	1160–1200		2500–3620
Carbonates; carboxyl-carbonates	1100–1500	1590–1600	
C=C aromatic (stretching)		1585–1600	
Quinones		1550–1680	
Carboxylic acids	1120–1200	1665–1760	2500–3300
Lactones	1160–1370	1675–1790	
Carboxylic anhydrides	980–1300	1740–1880	
C–H (stretching)			2600–3000

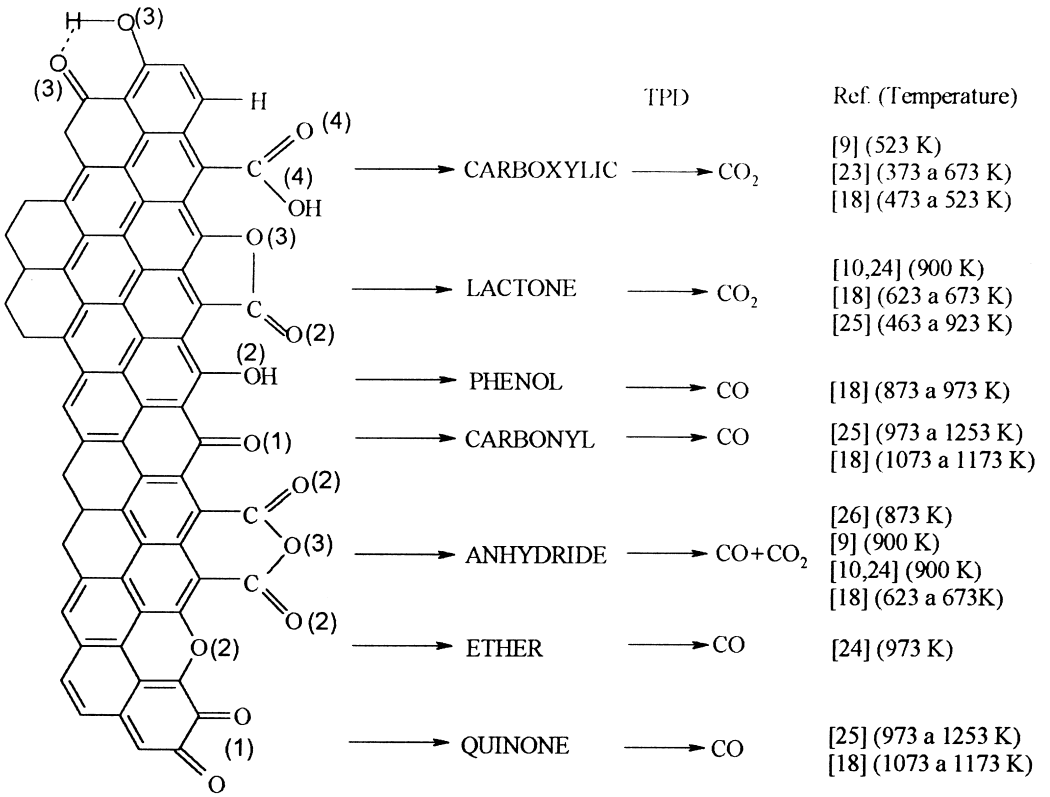

Fig. 1. Surface groups on carbon and their decomposition by TPD [9,10,18,23–26].

[29] was used to estimate the average micropore width of the smaller pores, using an affinity coefficient for nitrogen $\beta=0.34$.

The DRIFTS spectra were obtained without sample dilution in a Nicolet 510P spectrophotometer equipped with a diffuse reflectance attachment, by adding 256 scans at a resolution of 4 cm^{-1}. The samples were finely ground in a mortar for this analysis. Sample A8, where all surface groups were removed, was used as background; in this way, it was possible to obtain a better base-line correction and spectra with increased signal-to-noise ratio [30].

XPS analysis was performed at CEMUP (Centro de Materiais da Universidade do Porto) with a VG Scientific ESCALAB 200A spectrometer utilizing a non-monochromatized Mg Kα radiation (1253.6 eV). The vacuum in the analysis chamber was always $<1\times10^{-7}$ Pa.

The TPD profiles were obtained with a custom built set-up, consisting of a U-shaped tubular micro-reactor, placed inside an electrical furnace. The mass flow rate of the helium carrier gas (69 μg/s) and the heating rate of the furnace (5 K/min) were controlled with appropriate units. The amounts of CO and CO_2 desorbed from the carbon samples (0.1 g) were monitored with a SPECTRAMASS Dataquad quadrupole mass spectrometer.

The materials were further characterized by elemental and proximate analyses, with a CARLO ERBA EA 1108 Elemental Analyser and a Mettler TA 4000 thermal analyser, respectively.

3. Results and discussion

The results obtained for all samples by the various characterization techniques are shown in Tables 2–6, and

Table 2
Textural properties of all materials

Sample	V_{micro} (cm^3/g)	S_{me} (m^2/g)	W_{01} (cm^3/g)	W_{02} (cm^3/g)	L_1 (nm)
A1	0.372	126	0.347	0.029	0.91
A2	0.442	150	0.403	0.036	1.1
A3	0.497	149	0.450	0.045	1 2
A4	0.537	167	0.459	0.083	1.4
A5	0.575	173	0.445	0.146	1.6
A6	0.564	186	0.543	0.028	1.2
A7	0.557	178	0.536	0.028	1.3
A8	0.546	164	0.514	0.034	1.1
A9	0.592	217	0.522	0.077	1.3
A11	0.393	146	0.364	0.030	0.91
A12	0.388	157	0.355	0.034	0.94

Table 3
Proximate and elemental analyses of all materials

Sample	Proximate analysis				Elemental analysis			
	Moisture (wt%)	Volatiles (wt%)	C_{fixed} (wt%)	Ash (wt%)	C (wt%)	H (wt%)	N (wt%)	O (wt%)
A1	3.91	6.76	86.53	2.80	95.23	0.40	0.48	3.89
A2	1.06	10.13	85.59	3.26	92.77	0.25	0.41	6.56
A3	1.89	13.95	81.21	2.95	90.96	0.28	0.45	8.31
A4	1.77	17.75	77.72	2.75	89.72	0.29	0.64	9.34
A5	5.19	19.50	71.51	3.81	86.34	0.31	0.54	12.82
A6	2.17	12.81	81.52	3.51	92.72	0.35	0.65	6.27
A7	0.59	5.82	90.10	3.49	96.07	0.42	0.54	2.96
A8	1.83	3.19	90.98	3.99	98.10	0.20	0.73	0.97
A9	1.78	14.80	79.44	3.98	87.88	0.60	2.61	8.90
A11	3.26	7.30	87.52	1.92	85.79	0.87	1.06	12.28
A12	2.64	7.93	87.47	1.96	94.21	0.40	0.54	4.86

Table 4
XPS results for the O1s region, values given in % of the total amount

Sample	Binding energy (eV)				O_{total}	C_{total}	N	O_t/C_t
	531.1[a]	532.3[a]	533.3[a]	534.2[a]				
A1	1.90	2.08	1.66	0.81	6.46	93.51	n.d.	0.069
A2	2.57	1.38	3.38	0	7.33	92.67	n.d.	0.079
A3	3.41	1.66	4.49	0	9.55	90.45	n.d.	0.106
A4	4.605	2.18	6.06	0	12.83	87.17	n.d.	0.147
A5	4.86	3.66	6.99	0	15.51	84.51	n.d.	0.183
A6	2.74	2.31	3.69	0	8.74	91.26	n.d.	0.096
A7	1.69	1.46	1.25	0	4.40	95.60	n.d.	0.046
A8	0.86	1.34	1.11	0	3.31	96.68	n.d.	0.034
A9	4.26	1.36	5.93	0	11.55	85.08	3.37	0.136
A11	3.87	5.04	3.41	1.05	13.37	86.63	n.d	0.154
A12	2.22	3.86	4.30	2.00	12.38	87.62	n.d.	0.141

[a] Oxygen atoms of the relevant surface functional groups as shown in Fig. 1.

will be analysed and discussed in three stages: (a) General characterization, with emphasis on the different oxidation methods (samples A1, A4, A9, A11, A12); (b) Heat-treatments at different temperatures (samples A4, A6, A7, A8); and (c) Different degrees of oxidation by the same treatment (samples A1, A2, A3, A4, A5).

Table 5
Amounts of CO and CO_2 released, obtained by integration of the areas under the TPD peaks of the ROX activated carbon before and after different oxidative treatments

Sample	CO_2 (μmol/g)	CO (μmol/g)	CO/CO_2
A1	156	743	4.75
A2	214	3254	15.2
A3	265	3919	14.8
A4	351	4806	13.7
A5	534	6252	11.7
A9	200	3536	17.7
All	1104	2702	2.45
A12	420	1321	3.15

3.1. Different oxidation treatments

3.1.1. Textural characterization

The textural properties of all materials are collected in Table 2, while some of the nitrogen adsorption isotherms are shown in Fig. 2. It may be concluded that the liquid phase treatments have no significant impact on the texture of the carbon materials (A11 and A12 vs. A1), while gas phase oxidation increases the micropore volume, the

Table 6
Amounts of CO and CO_2 released, obtained by integration of the areas under the TPD peaks of the carbons before (sample A4) and after heat treatments at different temperatures (samples A6–A8)

Sample	CO_2 (μmol/g)	CO (μmol/g)	CO/CO_2
A4	351	4806	13.7
A6	88.9	3017	33.9
A7	67.6	581	8.59
A8	35.4	133	3.77

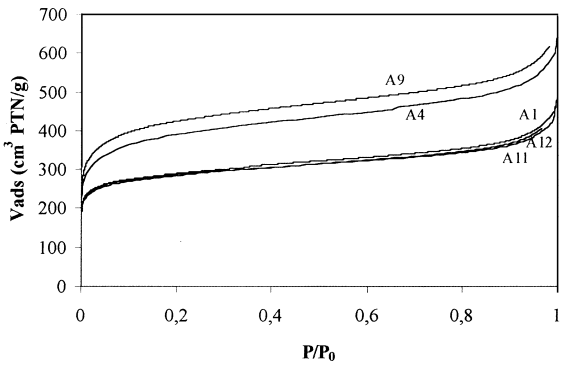

Fig. 2. Nitrogen adsorption isotherms at 77 K on the ROX activated carbon before and after different oxidative treatments.

mesopore surface area and the average width of the micropores (A4 and A9 vs. A1). These changes increase as the degree of oxidation increases (A1 vs. A2, A3, A4 and A5). In particular, the volume of the larger micropores (W_{02}) increases remarkably for higher degrees of B.O. (A4, A5). The samples which were submitted to thermal treatments under inert atmosphere (A6, A7, A8) do not show significant textural differences with respect to the parent material, A4.

It is generally reported that the liquid phase oxidations do not change significantly the texture of the activated carbons [7], although under more drastic conditions (concentrated acid, heating until complete evaporation) a decrease in surface area and pore volume has been observed while the average micropore width increases, due to the collapse of the pore walls [31]. In the gas phase oxidations the pore volume increases with burn-off, but it may be expected that, for higher degrees of oxidation, there will be a decrease first in the micropore volume and subsequently in the mesopore volume, due to the collapse of the pores [32].

3.1.2. Proximate and elemental analyses

The proximate and elemental analyses of the carbon samples before and after different oxidative treatments are shown in Table 3. It is apparent that the gas phase treatments lead to a substantial increase in the volatile matter content (samples A4, A9), while the liquid phase treatments originate only a modest increase in this parameter (A11, A12). Since the volatiles include the products released by the surface groups that decompose up to 1223 K, it is obvious that the gas phase treatments are the most effective. This is accompanied by a slight increase in ash content (due to carbon burn-off), whereas some ash is removed by the liquid phase treatments (which, by the way, do not cause any significant carbon burn-off). The increase in oxygen content is also observed by elemental analysis, although the result for A11 seems suspicious. The increase in nitrogen content is noticeable for samples A11 and especially A9. When comparing A4 with the heat-treated samples (A6, A7, A8), a gradual decrease in volatile matter and oxygen content is observed as the temperature increases.

3.1.3. Surface analysis by XPS

Table 4 shows the results obtained by XPS. The amounts determined for C, O, N were calculated from the corresponding peak areas divided by the appropriate sensitivity factors (1.000 for C, 2.850 for O and 1.770 for N [33]). The ratio of total oxygen to total carbon, O_t/C_t, which indicates the degree of surface oxidation, is also included. The reconstruction of the O1s peak gives additional information on the nature of the surface oxygen groups. The functionalities shown in Fig. 1 will contribute with peaks located at 531.1 eV (1), 532.3 eV (2), 533.3 eV (3) and 534.2 eV (4), in addition to chemisorbed water, at 535.9 eV [18]. The peaks were deconvoluted by using a sum of Lorentzian-Gaussian functions, fixing the width at half-height equal to 2.0 eV and allowing the position of the peak center to vary within ± 0.2 eV of the reported value [34].

All treated samples show an increase in the oxygen content. It is observed that the gas phase treatments (A4 and A9) increase mainly the groups (1) and (3), carbonyl/quinone and cetoenol, respectively, while the liquid phase treatments (A11 and A12) increase groups (2) and (4), hydroxyl+anhydrides and carboxylic acids, respectively. By comparing A4 with the heat-treated samples (A6, A7, A8), one can observe the gradual decrease in all types of surface oxygen groups. However, the total oxygen content of A8 is too high, probably reflecting the effect of surface re-oxidation by exposure to the atmosphere during sample handling.

3.1.4. TPD

Fig. 3 shows the TPD spectra of the ROX activated carbon before and after the different oxidative treatments. In all cases, an increase in the amount of surface oxygen groups is evidenced by the increase of the CO and CO_2 peaks. The CO_2 spectra are quite distinct: Thus, the liquid phase treatments increase the CO_2 evolution at low temperatures (from 373 to 673 K), while oxidation in the gas phase induces a CO_2 peak at higher temperatures. In the later case, the small peak at low temperature shown by the original carbon is no longer observed, as a result of the higher temperature used in this treatment (698 K). The TPD peaks can be tentatively assigned to the different functional groups by comparison with the data summarized in Fig. 1, taken from the available literature. The first CO_2 peak may be undoubtedly attributed to carboxylic acid functions, while the higher temperature CO_2 peak shows a shoulder at about 820 K and a maximum at about 930 K, which may result from carboxylic anhydrides and lactones. The gas phase treatment gives much more CO than the nitric acid treatment, but in both cases the TPD composite peaks show two maxima at around 900 K and 1070 K,

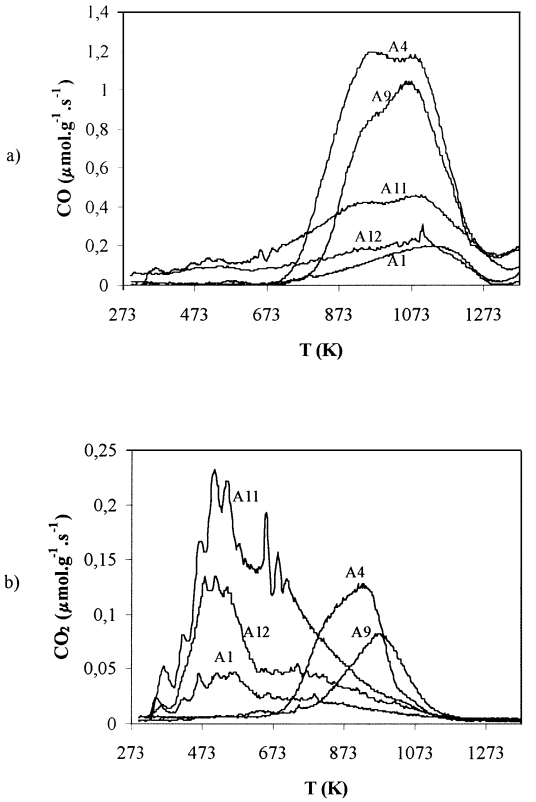

Fig. 3. TPD spectra before and after different oxidizing treatments: (a) CO evolution; (b) CO_2 evolution.

which may originate from phenols, ethers and carbonyls/quinones. Table 5 shows the amounts of CO and CO_2 released, obtained by integration of the areas under the TPD peaks, together with the ratio CO/CO_2. This ratio increases significantly after the gas-phase treatments (A4, A9), and decreases slightly after the liquid-phase treatments (A11, A12).

These results are consistent with an increase in carboxylic acid groups after nitric acid treatment, whereas gas phase oxidation increases anhydride, lactone, phenol and carbonyl/quinone surface groups. Both the TPD results and the proximate analyses show an increase in surface groups according to the sequence A1<A12<A11<A9<A4. The same is observed by elemental analysis, with the exception of A11, as noted above.

The XPS results are not directly comparable with the other techniques, since only the uppermost layers (10–15 nm) are analysed. The results suggest that the liquid phase treated materials may be more oxidized on the surface than in the bulk.

3.2. Heat-treated samples

Fig. 4 shows the DRIFTS spectra recorded for one of the carbons before (sample A4) and after heat treatments at different temperatures (samples A6, A7 and A8), while the corresponding TPD spectra are shown in Fig. 5.

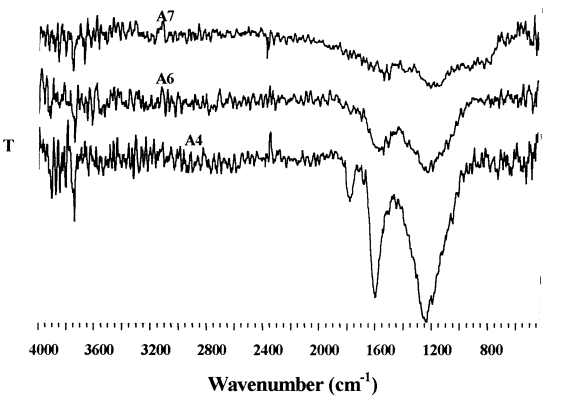

Fig. 4. DRIFTS spectra recorded for one of the carbons before (sample A4) and after heat treatments at different temperatures (samples A6 and A7).

Table 1 shows the infra-red bands which can be associated with different oxygen functional groups on carbon materials [14]. Inspection of Fig. 4 shows that there

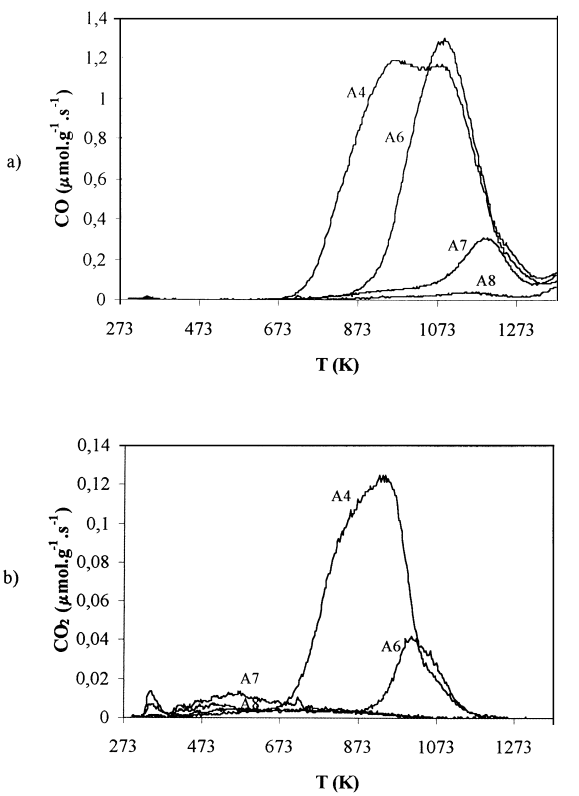

Fig. 5. TPD spectra for one of the carbons before (sample A4) and after heat treatments at different temperatures (samples A6–A8): (a) CO evolution; (b) CO_2 evolution.

are three bands of interest: one at 1750 cm^{-1}, associated with C=O stretching in lactones and carboxylic anhydrides, one at 1600 cm^{-1} associated with quinone and ceto-enol groups [35], and a broad band centered around 1250 cm^{-1} associated with C–O stretching in ethers, lactones, phenols and carboxylic anhydrides.

The band at 1750 cm^{-1}, associated with carboxylic anhydrides and lactones, disappears when heating to 873 K (A6); the two other bands decrease in sample A7.

Inspection of Fig. 5 shows that the shoulder in the CO peak disappears in sample A6, while in the CO_2 spectrum only a small peak is left at high temperatures. Sample A7 does not yield any CO_2, and only a small peak is left in the CO spectrum. All groups have disappeared from sample A8. Table 6 gives the CO and CO_2 contents of these samples determined from the TPD spectra.

By coupling together these observations (Figs. 4 and 5), it may be concluded that heating up to 873 K removes the carboxylic anhydrides and most of the lactones; some phenol groups are also removed, as shown by the decrease in intensity of the characteristic DRIFTS bands and by the decrease in the CO TPD peak. At 1023 K the lactones have been completely removed (no CO_2 peak), together with phenols and some carbonyls which reflect in the decrease of the bands at 1250 and 1600 cm^{-1}. Some carbonyls and ethers which were left are completely removed at 1373 K, as shown both by the absence of a CO peak in the TPD, and any bands in DRIFTS.

3.3. Samples oxidized in the gas phase to different extents

The TPD spectra obtained for samples A1, A2, A3, A4 and A5 are shown in Fig. 6, showing a gradual increase both in CO and CO_2 released as the extent of oxidation increases. However, the CO peak increases much more than the CO_2, leading to a very large increase in the CO/CO_2 ratio (cf. Table 5): a three-fold increase is observed in going from the original sample (A1) to the sample with the lower degree of oxidation (A2), decreasing slowly thereafter (A2 to A3, A4, A5). Similar behaviour was reported by Otake and Jenkins [9] with an activated carbon obtained from a phenol-formaldehyde resin.

It is also interesting to consider the changes observed in the shape of the CO peak as function of the degree of oxidation of the carbon (Fig. 6a). In effect, the high temperature shoulder is more prominent at low burn-off (sample A2) but the low temperature shoulder increases with the extent of oxidation and becomes the most intense in sample A5. This can be interpreted in terms of the mechanism for carbon gasification proposed by Zhuang et al. [36]

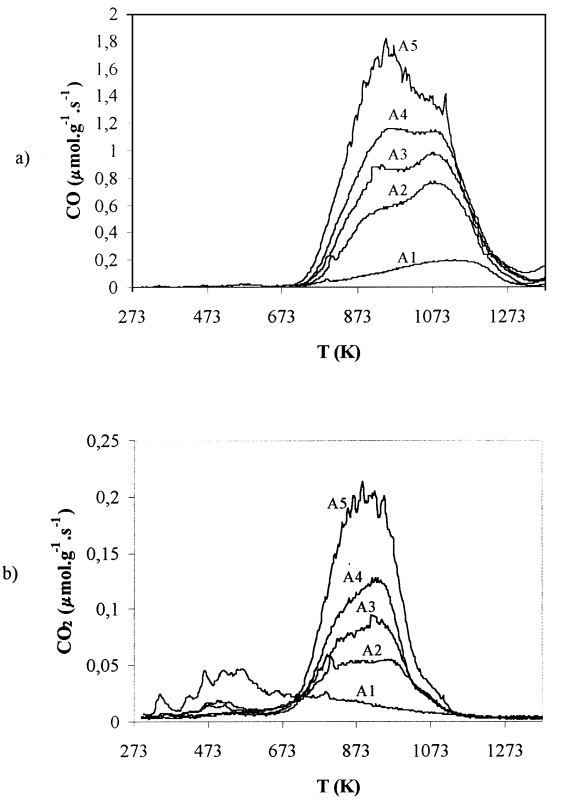

Fig. 6. TPD spectra for the samples oxidized in the gas phase (5% O_2 in N_2) to different extents: (a) CO evolution; (b) CO_2 evolution.

$$C_f + O_2 \rightarrow \text{carbonyls, ethers}(+ CO) \quad (1)$$

$$C_f + O_2 \rightarrow \text{lactones, anhydrides} \quad (2)$$

$$C_f + \text{carbonyls, ethers} + O_2 \rightarrow CO_2 + \text{CO or carbonyls, ethers} \quad (3)$$

$$C_f + \text{carbonyls, ethers} + O_2 \rightarrow \text{lactones, anhydrides} \quad (4)$$

$$\text{lactones, anhydrides} \rightarrow CO_2(+ CO) + 2C_f \quad (5)$$

$$\text{carbonyls, ethers} \rightarrow CO + C_f \quad (6)$$

where C_f is a free active site on the carbon surface. The phenol groups, not considered by Zhuang et al. [36], should be included in these reactions. Reactions (1) and (3) were assumed predominant. Reactions (5) and (6), corresponding to the decomposition of the surface groups, should be negligible at the oxidation temperature used (698 K).

Reactions (1) and (3) are much more important than (2) and (4), since the amount of CO released by TPD (reaction 6) is much larger than the CO_2 (reaction 5) indicating that there are much more carbonyl, ether and phenol groups (reaction 1 and 3) than lactones and anhydrides (reactions 2 and 4). In effect, Table 5 shows that the ratio CO/CO_2 is always higher than 10.

Table 7
Comparison between the oxygen concentrations (wt%) obtained by different techniques

Sample	Elem. anal.	TPD	XPS
A2	6.56	6.63	9.54
A3	8.31	8.01	12.3
A4	9.34	9.91	16.4
A5	12.8	13.2	19.7

The shape of the CO peak can be analysed in terms of this mechanism as follows:

At low degrees of oxidation, the shoulder at 1100 K (carbonyl, ether) is higher than the shoulder at 900 K (phenol, anhydrides), indicating that reaction (1) prevails. However, as the concentration of carbonyl, ether and phenol groups increases on the surface, reaction (4) becomes favoured. This originates anhydrides, one of the components of the CO peak at 900 K. Thus, for high degrees of oxidation, there is a larger increase in the 900 K shoulder with respect to the 1100 K shoulder.

It is particularly instructive to compare the results obtained by TPD with those of the other techniques for samples A2, A3, A4 and A5, which have all been processed at the same temperature (698 K). It may be observed from Tables 7 and 8 that both the concentration of oxygen obtained by elemental analysis, and the concentration of volatiles determined by proximate analysis, correlate quite well with the TPD results. Thus, the volatile matter of these samples corresponds to the amounts of CO and CO_2 desorbed. The XPS results for oxygen are higher, indicating that the surface is more oxidized than the bulk.

In order to determine the amount of each surface group, the deconvolution of the CO and CO_2 TPD spectra of the gas phase oxidized carbons was based on the following assumptions, suggested by the results reported above: (a) The CO_2 spectra are decomposed into two contributions, corresponding to carboxylic anhydrides and lactones. There is not any low temperature CO_2 evolution, since these samples were processed at a temperature higher than the decomposition of carboxylic acids. (The small peaks shown by A2 and A3 may result from exposure to the atmosphere [23]). Although most authors do not distinguish between lactones and anhydrides, quoting the same decomposition temperature for them [10,18], in this work it is assumed that the first component corresponds to anhydrides (CO_2 peak #1) and the second corresponds to the lactones (CO_2 peak #2).

Table 8
Comparison between the volatile matter (proximate analysis) and the amounts of $CO+C0_2$ released by TPD (expressed in wt%)

Sample	Volatiles	$CO+CO_2$
A2	10.1	10.0
A3	14.0	12.1
A4	17.8	15.0
A5	19.5	19.9

(b) The carboxylic anhydrides decompose by releasing one CO and one CO_2 molecule [37]. Thus, the first component in the CO spectra corresponds to the carboxylic anhydrides, with a peak of the same shape and equal magnitude of the CO_2 peak #1 (CO peak #1). This peak is defined from the deconvolution of the CO_2 spectra.

(c) In addition to the carboxylic anhydrides (CO peak #1), the CO spectra include contributions from phenols (CO peak #2) and carbonyl/quinones (CO peak #3) [18]. This sequence of decomposition temperatures, first phenols, then carbonyl/quinones, is justified by the higher stability of the later groups.

(d) It is assumed that secondary reactions are negligible. For instance, the Boudouard reaction $CO(g)+C[O]=C_f+CO_2$ (g), where C_f is a free active site and C[O] is a surface oxygen complex, would lead to the release of CO_2 at about 1000 K at the expense of CO [38,39]. The absence of such reactions under the experimental conditions used in the present work was confirmed by performing the TPD at different flow rates of the carrier gas.

(e) A multiple gaussian function was used for fitting each of the TPD spectra, taking the position of the peak center as initial estimate. The numerical calculations were based on a non-linear routine which minimized the square of the deviations, using the Simplex method to perform the iterations. The use of gaussian functions is justified by the shape of the TPD peaks, which are a result of a continuous random distribution of binding energies of the surface groups [40].

(f) In the CO_2 spectra, the width at half-height was taken as the same for both peaks. This restriction is needed when the spectra do not present definite shoulders, such as sample A5 (in which case one single peak would describe the situation well). In the other cases, the widths at half-height obtained when the restriction is removed are quite similar, which justifies the procedure. This restriction does not affect significantly the amounts obtained for the CO components #2 and #3.

This deconvolution procedure proved to fit the data quite well, as shown in Fig. 7 for the CO and CO_2 TPD spectra of samples A2, A3, A4 and A5.

Table 9 gives the results obtained, where T_M is the temperature of the peak maximum, W is the width of the peak at half-height and A is the integrated peak area. It can be observed that all the fits, for carbons oxidized to different extents and containing quite different amounts of surface groups, give approximately the same values of T_M and W for each component; moreover, the T_M values correspond closely to the peak maxima observed in the TPD spectra, and are within the range of values reported in the literature (cf. Fig. 1).

Thus, the decomposition temperatures found were circa 820 K for anhydrides, 940 K for lactones, 905 K for phenols and 1080 K for carbonyls/quinones.

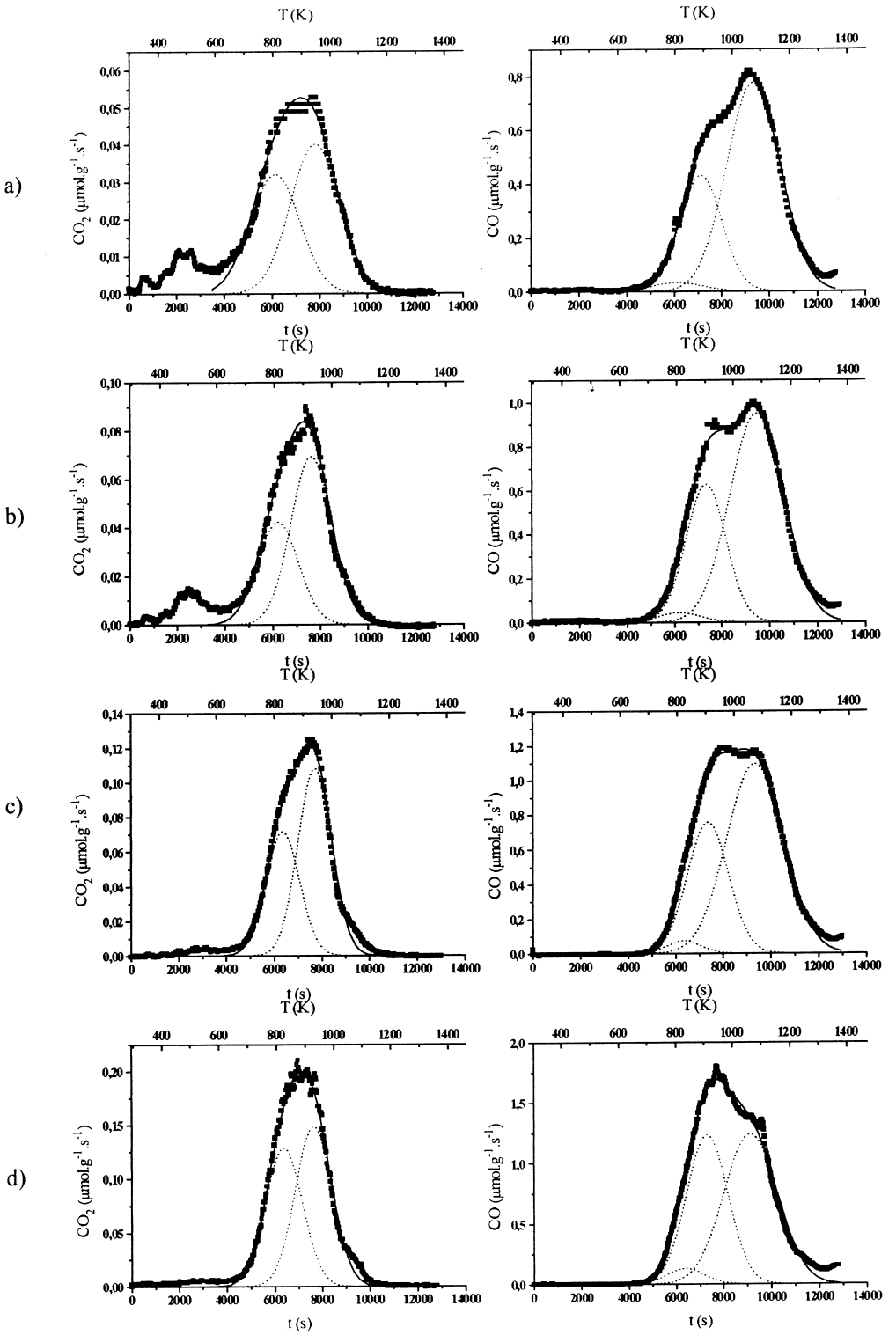

Fig. 7. Results of the deconvolution of TPD spectra using a multiple Gaussian function. (a) Sample A2, (b) Sample A3, (c) Sample A4, (d) Sample A5. (■, TPD experimental data; - - -, individual peaks; ———, sum of individual peaks).

Table 9
Results of the deconvolution of TPD spectra using a multiple Gaussian function

Sample	CO_2						CO								
	Peak #l			Peak #2			Peak #1			Peak #2			Peak #3		
	T_M (K)	W (K)	A (μmol/g)	T_M (K)	W (K)	A (μmol/g)	T_M (K)	W (K)	A (μmol/g)	T_M (K)	W (K)	A (μmol/g)	T_M (K)	W (K)	A (μmol/g)
A2	810±30	172±20	83.2±37	949±24	172±17	104±37	810	172	83.2	892±4	147±4	952±56	1078±3	186±4	2174±57
A3	812±53	143±35	90.5±85	929±32	143±24	149±85	812	143	90.5	904±3	140±3	1321±69	1107±3	189±4	2694±70
A4	823±9	118±8	127±21	936±6	118±6	192±21	823	118	127	907±3	145±4	1643±128	1073±4	198±5	3263±130
A5	836±17	128±11	248±83	941±15	128±11	287±83	836	128	248	912±7	145±7	2694±352	1064±10	186±11	3474±355

In a recent publication, Calo et al. [37] studied the influence of hydrogen on the TPD of surface complexes on activated carbon. They considered that the CO_2 peak results only from anhydrides, and therefore subtracted it totally from the CO peak. In spite of this difference, these authors found for CO peak #2 $T_M = 955$ K and $W = 144$ K, and for CO peak #3 $T_M = 1100$ K and $W = 134$ K. Considering that a higher heating rate was used by these authors (10 K/min), the agreement with the present results is quite reasonable.

4. Conclusions

It has been shown that gas phase oxidation of activated carbons increases mainly the concentration of hydroxyl and carbonyl surface groups, while oxidation in the liquid phase increases especially the concentration of carboxylic acids.

In terms of total oxygen content, the results obtained by TPD agree quite well with the elemental analyses of the oxidized materials. Higher amounts of oxygen are determined by XPS, indicating that the concentration of the functional groups is higher at the surface of the particles. The results obtained by TPD agree well with the qualitative observations by DRIFTS.

The amounts of the different surface groups can be estimated by deconvolution of the TPD spectra. It has been shown that a multiple gaussian function adequately fits the data. Moreover, the parameters obtained for each fit correspond to the features observed in the experimentally determined TPD spectra.

Acknowledgements

This work was carried out with support from the PRAXIS XXI Programme (contract numbers 2/2.1/BIO/34/94 and PCEX/C/QUI/98/96). M.F.R. Pereira and M.M.A. Freitas acknowledge the grants received under the same programme. The authors are indebted to Dr. Carlos M. Sá (CEMUP) for assistance with XPS analysis, and to NORIT N.V., Amersfoort, The Netherlands, for providing the activated carbon.

References

[1] Rodriguez-Reinoso F. Carbon 1998;36:159.
[2] Wigmans T. In: Figueiredo JL, Moulijn JA, editors, Carbon and Coal Gasification, Dordrecht, The Netherlands: Martinus Nijhoff Publishers, 1986, pp. 559–599.
[3] Boehm HP. In: Eley DD, Pines H, Weisz PB, editors, Advances in Catalysis, Vol. 16, New York: Academic Press, 1966, pp. 179–274.
[4] Donnet JB. Carbon 1968;6:161.
[5] Boehm HP, Diehl E, Heck W. In: Proc. 2nd London Carbon and Graphite Conf., London, UK, 1965, p. 369.
[6] Bandoz TJ, Jagiello J, Schwarz JA. An Chem 1992;64:891.
[7] Noh JS, Schwarz JA. Carbon 1990;28:675.
[8] Vinke P, Van der Eijk M, Verbree M, Voskamp AF. Carbon 1994;32:675.
[9] Otake Y, Jenkins RG. Carbon 1993;31:109.
[10] Zhuang Q-L, Kyotany T, Tomita A. Energy and Fuels 1994;8:714.
[11] Park SHP, McClain S, Tian ZR, Suib SL, Karwacki C. Chem Mater 1997;9:176.
[12] Biniak S, Szymanski G, Siedlewski J, Swiatkowski A. Carbon 1997;35:1799.
[13] Ishizaki C, Marti I. Carbon 1981;19:409.
[14] Fanning PE, Vannice MA. Carbon 1993;31:721.
[15] Zawadzki J. In: Thrower PA, editor, Chemistry and Physics of Carbon, Vol. 21, New York: Marcel Dekker, Inc, 1988, pp. 147–386.
[16] Papirer E, Dentzer J, Li S, Donnet J. Carbon 1991;29:69.
[17] Boehm HP. High Temperatures-High Pressures 1990;22:275.
[18] Zielke U, Huttinger KJ, Hoffman WP. Carbon 1996;34:983.
[19] Wiertz V, Bertrand P. In: Proceedings of the International Conference on Polymer-Solid Interfaces, ICPSI-2, Namur, Belgium, 1996.
[20] Falconer JL, Schwarz JA. Catal Rev-Sci Eng 1983;25:141.
[21] Boehm HP, Bewer G. In: Proc. 4th London Carbon and Graphite Conf, London, UK, 1974, p. 344.
[22] Boehm HP. Carbon 1994;32:759.

[23] Zhuang Q-L, Kyotany T, Tomita A. Carbon 1994;32:539.
[24] Zhuang Q-L, Kyotany T, Tomita A. Ext. Abstracts Carbon '94, Granada, Spain, 1994, p. 466.
[25] Marchon B, Carrazza J, Heinemann H, Somorjai GA. Carbon 1988;26:507.
[26] Driel J. In: Capelle A, de Vooys F, editors, Activated Carbon – A Fascinating Material, The Netherlands: Norit, Amersfoort, 1983, pp. 40–57.
[27] Rodriguez-Reinoso F, Martin-Martinez JM, Prado-Burguete C, McEnaney B. J Phys Chem 1987;91:515.
[28] Linares-Solano A. In: Figueiredo JL, Moulijn JA, editors, Carbon and Coal Gasification, Dordrecht, The Netherlands: Martinus Nijhoff Publishers, 1986, pp. 137–78.
[29] Stoeckli HF, Ballerini L, De Bernardini S. Carbon 1989;27:501.
[30] Venter JJ, Vannice MA. Carbon 1988;26:889.
[31] Moreno-Castilla C, Carrasco-Marín F, Maldonado-Hódar FJ, Rivera-Utrilla J. Carbon 1998;36:145.
[32] Rodríguez-Reinoso F. In: Lahaye J, Ehrburger P, editors, Fundamental Issues in Control of Carbon Gasification Reactivity, Dordrecht, The Netherlands: Kluwer Academic Publishers, 1991, pp. 533–571.
[33] Ikeo N, Iijma Y, Niimura N, Sigematsu M, Tazawa T, Matsumoto S, Kojima K, Nagsawa Y. Handbook of X-ray Photoelectron Spectroscopy, JEOL, 1991.
[34] Desimoni E, Casella GI, Morone A, Salvi AM. Surface and Interface Analysis 1990;15:627.
[35] Lien-Vien D, Colthup NB, Fateley WG, Grasselli JG. In: The Handbook of Infrared and Raman Characteristic Frequencies of Organic Molecules, S. Diego, Toronto: Academic Press, Inc, 1991, pp. 117–54, Chapter 9.
[36] Zhuang Q-L, Kyotany T, Tomita A. Energy and Fuels 1995;9:630.
[37] Calo JM, Cazorla-Amorós D, Linares-Solano A, Román-Martinez MC, Salinas-Martínez De Lecea C. Carbon 1997;35:543.
[38] Hall PJ, Calo JM, Lilly WD. In: McEnaney B, Mays TJ, editors, Proceedings of the International Conference on Carbon, Carbon' 88, Bristol, UK: IOP Publishing Co, 1988, p. 77.
[39] Hall PJ, Calo JM. Energy and Fuels 1989;3:370.
[40] Calo JM, Hall PJ. In: Lahaye J, Ehrburger P, editors, Fundamental Issues in the Control of Carbon Gasification Reactivity, Dordrecht, The Netherlands: Kluwer Academic Publishers, 1991, pp. 329–368.